11th World Congress on Computational Mechanics (WCCM XI)
5th European Conference on Computational Mechanics (ECCM V)
6th European Conference on Computational Fluid Dynamics (ECFD VI)
E. Oñate, J. Oliver and A. Huerta (Eds)

SPECIFIC ASPECTS OF NUMERICAL SIMULATION OF CIVIL ENGINEERING STRUCTURES WITH CROSS SECTION SHAPE CLOSE TO RECTANGULAR

IRINA N. AFANASYEVA[*], ANTON R. USMANOV[*], ALEXANDR M. BELOSTOTSKIY[*] AND SERGEY I. DUBINSKY[*]

[*] Department of Computer Science and Applied Mathematics,
Research & Educational Center of Computational Simulation,
Moscow State University of Civil Engineering (MGSU),
26, Yaroslavskoe Shosse, 129337, Moscow, RUSSIA
e-mail: niccm@mgsu.ru

Key Words: *Civil Engineering, Computational Fluid Dynamics (CFD), Numerical Simulation, Turbulence models, Large Eddy Simulation, Detached Eddy simulation, Rectangular Cylinder.*

Abstract. Present paper is devoted to the specific aspects of the numerical simulation of the aerodynamics of buildings and structures, which shape is similar to a rectangular cylinder (e.g., bridges, high-rise buildings etc.) for obtaining authentic transient wind loads on them using Computational Fluid Dynamic (CFD) technologies. Comparison between the wind tunnel experimental data and the results of numerical simulation using LES and DES approaches was carried out. Specific aspects, rules and recommendations for the numerical simulation of civil engineering structures with cross sectional shape close to a rectangular were developed.

1 INTRODUCTION

For the considered civil structures wind loads are interesting as local wind loads on facades or as dynamic loads leading to resonance effects like galloping and flutter. From this point of view it would be more interesting and important to solve problem using Fluid Structure Interface (FSI) methods, but it is just a next step, because first of all it is necessary to obtain authentic transient wind loads on building and structures using Computational Fluid Dynamic (CFD) technologies.

All methods of fluid dynamics numerical simulation solve the Navier-Stockes equations. For the turbulence flow there are additional equations named as turbulence models: RANS (Reynolds Averaged Navier-Stokes), LES (Large Eddy Simulation) и DES (Detached Eddy Simulation) [1]. To use this approaches by right way and to obtain good results there are requirements according to numerical schemes, additional parameters and especially to mesh qualities. RANS turbulence models have proven itself in the definition of the mean velocity and pressure fields and leading load frequency and less demanding on the mesh quality as well. This fact is important for creating numerical grid for buildings and civil structures of complex form and allows to solve this kind of problem in a short timeframe. But to accurate estimation of dynamic loads and three-dimensional effects of flow around the obstacle it is necessary to use LES group of turbulence models.

The purpose of the research is to assess the applicability of such turbulence models as LES (Large Eddy Simulation) and DES (Detached Eddy Simulation) demands for high mesh qualities for civil structures and buildings of complex three-dimensional shape. Therefore, there is need for investigation of the grid resolution in the boundary layer (near the walls of obstacles), in the transverse direction to the cross section of structure and shape and quality of mesh in the domain. This kind of research will give understanding of “the cost” of the obtaining authentic results using LES approach, the limit of the mesh simplification near and around the object for DES approach and the value of an error using RANS turbulence models.

2 GOVERNING EQUATIONS

2.1 Unsteady RANS equations [1]

Substituting the averaged quantities into the original transport equations results in the Reynolds averaged equations given below (Eq. 1, Eq. 2):

$$\frac{\partial}{\partial t}(\rho\overline{u_j})+\frac{\partial}{\partial x_i}(\rho\overline{u_i}\cdot\overline{u_j})=-\frac{\partial\overline{p}}{\partial x_j}+\frac{\partial}{\partial x_i}\left[\mu\left(\frac{\partial\overline{u_i}}{\partial x_j}+\frac{\partial\overline{u_j}}{\partial x_i}\right)-\rho\overline{u'_i u'_j}\right] \tag{1}$$

$$\frac{\partial u_i}{\partial x_i}=0,\ \frac{\partial u'_i}{\partial x_i}=0, \tag{2}$$

where: ρ – the fluid density (ρ = *const* for an incompressible fluid or gas); μ – dynamic viscosity; p – the average pressure, the indices i = 1,2,3 and j = 1,2,3 correspond to the coordinates x, y, z. Shear (Reynolds) stress $\rho\overline{u'_i u'_j}$ are additional six unknowns ($\overline{u_i}$, $\overline{p}$) which are approximated as a rule by the Boussinesq's assumption (Eq. 3):

$$\rho\overline{u'_i u'_j} = -\mu_t\left(\frac{\partial\overline{u_i}}{\partial x_j}+\frac{\partial\overline{u_j}}{\partial x_i}\right)+\frac{2}{3}\rho k\delta_{ij} \tag{3}$$

The system of equations (Eq. 1, Eq. 2, Eq. 3) is not closed. To close this system semi-empirical relations (turbulence models) connecting additional unknowns (Reynolds stress) with time-averaged velocity components are imposed.

2.2 LES equations [1]

The governing equations for LES are obtained by filtering the time-dependent Navier-Stokes equations in the physical space. The filtering process effectively filters out the eddies whose scales are smaller than the filter width or grid spacing used in the computations. The resulting equations thus govern the dynamics of the large eddies.

The filtered incompressible momentum equation can be written in the following way (Eq. 4, Eq. 5):

$$\overline{\Phi}(x)=\frac{1}{V}\int_V \Phi(x')dx' \tag{4}$$

$$\frac{\partial\bar{U}_i}{\partial \mathrm{t}}+\frac{\partial}{\partial \mathrm{x_j}}\left(\bar{U}_i\bar{U}_j\right)=-\frac{1}{\rho}\frac{\partial\bar{p}}{\partial \mathrm{x_i}}+\frac{\partial}{\partial \mathrm{x_j}}\left(\nu\left(\frac{\partial\bar{U}_i}{\partial \mathrm{x_j}}+\frac{\partial\bar{U}_j}{\partial \mathrm{x_i}}\right)\right)-\frac{\partial\tau_{ij}}{\partial \mathrm{x_j}}-\left(\tau_{ij}-\frac{\delta_{ij}}{3}\tau_{kk}\right)=\nu_{SGS}\left(\frac{\partial\bar{U}_i}{\partial \mathrm{x_j}}+\frac{\partial\bar{U}_j}{\partial \mathrm{x_i}}\right) \tag{5}$$

The large scale turbulent flow is solved directly and the influence of the small scales is taken into account by appropriate subgrid-scale (SGS) models. The wall-adapted local eddy-viscosity model by Nicoud and Ducros (LES WALE model) are shown below (Eq. 6):

$$\begin{aligned}
\nu_{SGS} &= \left(c_w\Delta\right)^2\frac{\left(\bar{S}_{ij}^d\bar{S}_{ij}^d\right)^{\frac{3}{2}}}{\left(\bar{S}_{ij}\bar{S}_{ij}\right)^{\frac{5}{2}}+\left(\bar{S}_{ij}^d\bar{S}_{ij}^d\right)^{\frac{5}{4}}}\\
\bar{S}_{ij}^d &= \frac{1}{2}\left(\bar{g}_{ij}^2+\bar{g}_{ji}^2\right)-\frac{1}{2}\delta_{kk}\bar{g}_{kk}^2\\
\bar{g}_{ij} &= \frac{\partial\bar{U}_i}{\partial x_j}
\end{aligned} \tag{6}$$

2.3 DES equations [1]

DES is an attempt to combine elements of RANS and LES formulations in order to arrive at a hybrid formulation, where RANS is used inside attached and mildly separated boundary layers. Additionally, LES is applied in massively separated regions.

DES-SST formulation Strelets is shown below (Eq. 7, Eq.8):

$$\begin{aligned}
\varepsilon &= \beta^* k\omega = k^{\frac{3}{2}}/\left(C_{DES}\Delta < L_t\right)\\
\Delta &= \max(\Delta_i);\ L_t = \left(\sqrt{k}\right)/\beta^*\omega
\end{aligned} \tag{7}$$

where: k – turbulent kinetic energy; ω – turbulent frequency; ε – turbulent dissipation; L_t – turbulent length, Δ – local grid spacing; $C_{DES} = 0.61$.

The DES modification of Strelets can be formulated as a multiplier to the destruction term

in the k-equation:

$$\varepsilon = \beta^* k\omega \rightarrow \beta^* k\omega \cdot F_{DES}$$
$$F_{DES} = \max\left(\frac{L_t}{C_{DES}\Delta}, 1\right) \tag{8}$$

The numerical formulation is also switched between an upwind biased and a central difference scheme in the RANS and DES regions respectively.

3 PROBLEM STATEMENT

The multivariate verification investigations were carried out at the world-known benchmark BARC [2], that is devoted to 1:5 prism aerodynamics research (Figure 1).

The used control parameters are the mean and standard deviation of the pressure coefficient (Eq. 9) along the prism side, the aerodynamic forces (Eq. 10) – drag, F_D, lift, F_L, and torque moment, M_Z (torque is meant evaluated with respect to the origin of the reference system) and Strouhal number (Sh) (Eq. 11). The comparison data was taken from wind tunnel experiment carried out by Bronkhorst [3].

$$C_{\bar{p}} = \frac{\bar{p}}{0.5\rho U_\infty^2}; C_{\sigma_p} = \frac{\sigma_p}{0.5\rho U_\infty^2} \tag{9}$$

$$C_{\bar{D}} = \frac{\bar{F}_D}{0.5\rho U_\infty^2}; C_{\sigma_D} = \frac{\sigma_D}{0.5\rho U_\infty^2};\ C_{\bar{L}} = \frac{\bar{F}_L}{0.5\rho U_\infty^2}; C_{\sigma_L} = \frac{\sigma_L}{0.5\rho U_\infty^2};\ C_{\bar{M}_Z} = \frac{\bar{M}_z}{0.5\rho U_\infty^2}; C_{\sigma_{M_Z}} = \frac{\sigma_{M_Z}}{0.5\rho U_\infty^2} \tag{10}$$

$$Sh = \frac{f_1 D}{U_\infty} \tag{11}$$

4 COMPUTATIONAL APPROACH

The computational domain matches to the wind tunnel working section described in [3] and is shown in Figure 1.

The computational mesh are unstructured in the *xy* plane and structured along the *z* axis. There is mesh refining in the area nearest to obstacle.

The investigation of the influence of the grid resolution in the boundary layer (near the walls of the rectangular), in the transverse direction (Z) to the cross section and the influence of the domain size in the transverse direction (Z) on the results. The main meshes parameters are listed in Table 1.

As "inlet" boundary conditions (Inlet) constant longitudinal velocity profile with a value of U_∞=7.5 m/s (Re=5e+4) and turbulence intensity It=0% (smooth flow) are imposed. Eddy Length Scale = 3 m. On the upper and lower boundaries - "No Slip Wall" (velocity components U=V=W=0). On the side boundaries "Periodic" boundary conditions are imposed. Neumann conditions on the normal component of stress tensor are imposed at the "outlet" boundaries. As initial conditions the results of steady state simulations are imposed.

The time step for the transient simulations is chosen as Δt=1e-004 s. For the steady state simulation RANS iteration are performed up to stabilization of the calculated parameters CX, CY, CMZ and achievement of desired level of residuals 1e-005. For the transient simulations iteration are performed up to achieving steady oscillatory regime.

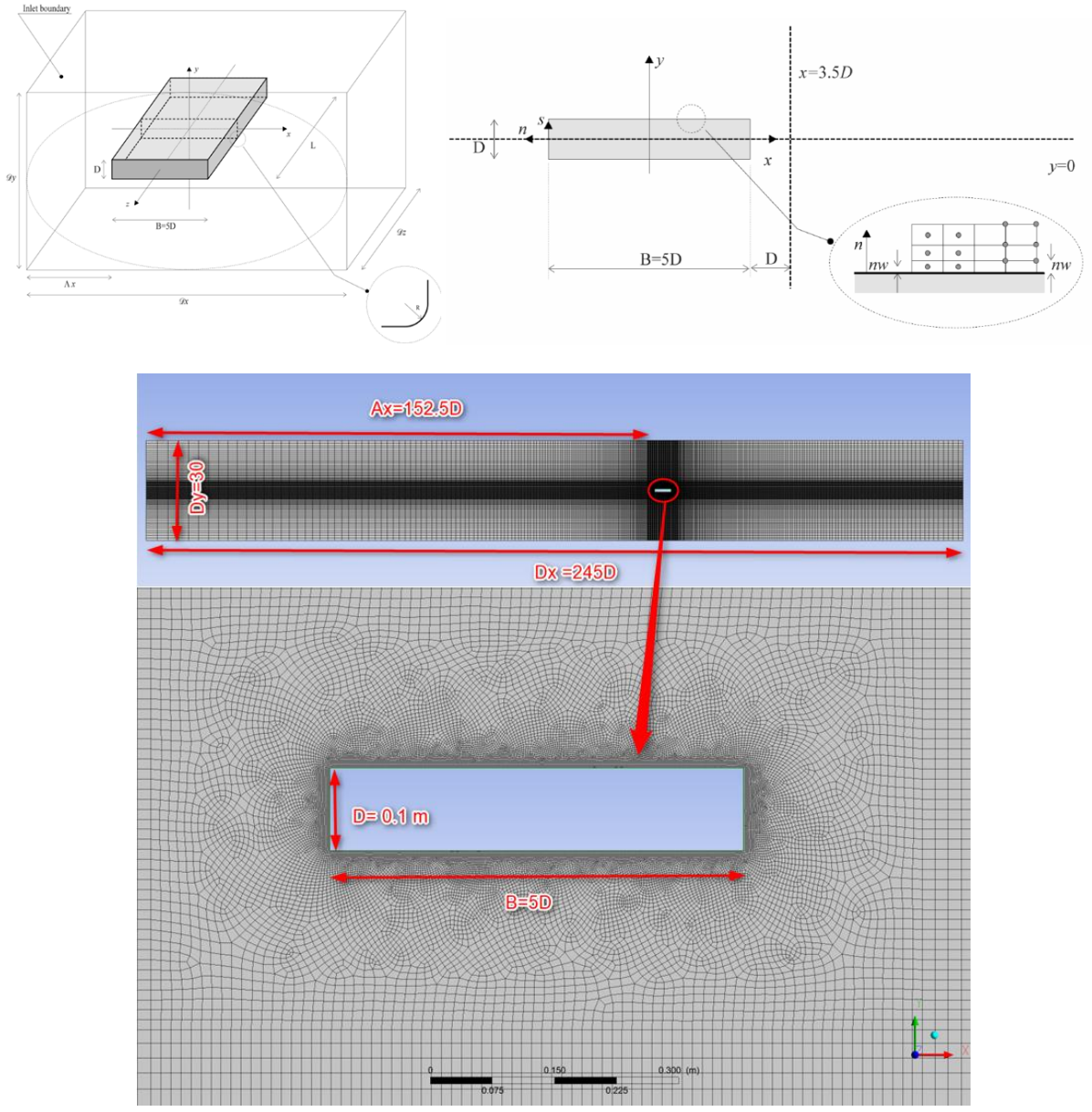

Figure 1: Geometry configurations and mesh topology (Case 14 in Table 1)

Table 1: Case setup

Case Number	Turb. Model	L/D	Nz	Ny	Nx	dz [m]	dy [m]	dx [m]	*nw* [m]	ratio_xy	ratio_zx	ratio_zy	y+
1	DES	0.333	5	54	269	0.00666	0.00186	0.00186	0.00186	1.0	3.6	3.6	40
2	DES	0.5	10	538	2688	0.00500	0.00019	0.00019	0.00019	1.0	26.9	26.9	4
3	LES	0.5	10	538	2688	0.00500	0.00019	0.00019	0.00019	1.0	26.9	26.9	4
4	DES	0.5	10	54	269	0.00500	0.00186	0.00186	0.00186	1.0	2.7	2.7	40
5	LES	0.5	20	215	1075	0.00250	0.00047	0.00047	0.00047	1.0	5.4	5.4	10
6	LES	0.5	40	215	1075	0.00125	0.00047	0.00047	0.00047	1.0	2.7	2.7	10
7	LES	0.5	5	538	2688	0.01000	0.00019	0.00019	0.00019	1.0	53.8	53.8	4
8	DES	1	10	215	1075	0.01000	0.00047	0.00047	0.00047	1.0	21.5	21.5	10
9	LES	1	10	215	1075	0.01000	0.00047	0.00047	0.00047	1.0	21.5	21.5	10
10	LES	1	10	22	108	0.01000	0.00465	0.00465	0.00465	1.0	2.2	2.2	100
11	DES	1	10	108	538	0.01000	0.00093	0.00093	0.00093	1.0	10.8	10.8	20
12	DES	1	10	538	2688	0.01000	0.00019	0.00019	0.00019	1.0	53.8	53.8	4
13	LES	1	10	538	2688	0.01000	0.00019	0.00019	0.00019	1.0	53.8	53.8	4
14	DES	1	10	54	269	0.01000	0.00186	0.00186	0.00186	1.0	5.4	5.4	40
15	LES	1	10	54	269	0.01000	0.00186	0.00186	0.00186	1.0	5.4	5.4	40
16	DES	1	10	43	215	0.01000	0.00233	0.00233	0.00233	1.0	4.3	4.3	50
17	DES	1	20	54	269	0.00500	0.00186	0.00186	0.00186	1.0	2.7	2.7	40
18	LES	1	80	215	1075	0.00125	0.00047	0.00047	0.00047	1.0	2.7	2.7	10
19	DES	4	40	54	269	0.01000	0.00186	0.00186	0.00186	1.0	5.4	5.4	40
20	DES	5	50	54	269	0.01000	0.00186	0.00186	0.00186	1.0	5.4	5.4	40
21	LES	1	10	215	1075	0.01000	0.00047	0.00047	0.00005	10.0	21.5	215.0	1
22	DES	0.5	5	54	269	0.01000	0.00186	0.00186	0.00186	1.0	5.4	5.4	40
23	DES	1	10	22	108	0.01000	0.00465	0.00465	0.00465	1.0	2.2	2.2	100
24	DES	1	10	72	358	0.01000	0.00140	0.00140	0.00140	1.0	7.2	7.2	30
25	DES	2	20	54	269	0.01	0.00186	0.00186	0.00186	1	5.4	5.4	40
26	DES	3	30	54	269	0.01	0.00186	0.00186	0.00186	1	5.4	5.4	40

where: Nz, Ny, Nx – numbers of divisions along rectangular edges in Z, Y, X directions, respectively; dz, dy, dx – element sizes along rectangular edges in Z, Y, X directions, respectively, [m]; *nw* – normal distance from the wall of the first node layer closest to the wall [m]; ratio_xy – element size ratio: dx/dy; ratio_zx – element size ratio: dz/dx;, ratio_zy – element size ratio: dz/dy.

5 RESULTS AND DISCUSSION

5.1 LES simulations

The obtained results of LES simulations are presented in Table 2 and Figures 2.

The investigations showed significant influence of the grid resolution in the boundary layer (y+) on the mean and standard-deviation values distribution of pressure coefficients (C_p, $C_{\sigma p}$). The values of y+ more than 10 lead to overestimate maximum values of $C_{\sigma p}$, that appear at the wrong area of the upper and lower surfaces of the rectangular because the "separation bubble" and "main vortex" [6] are formed incorrectly.

The size of domain in the transverse direction (Z) L=1D is optimal in terms of computational cost and reliability of results.

The more regular shape of cells near the walls of the structure are created, the better results are obtained. The results are closest to experiments when Nz=80 (ratio_xy=1, ratio_zx=2.7, ratio_zy=2.7).

The main aerodynamic integral parameters (Table 2) seem not to be sensitive to grid resolution contrary to local parameters and are similar to the other studies [4, 5].

Table 2: Mean (C_D, C_L), standard-deviation ($C\sigma_D$, $C\sigma_L$) and Strouhal number (Sh) values of drag and lift coefficients for several LES simulations

Case Number	C_D	$C\sigma_D$	C_L	$C\sigma_L$	C_{Mz}	$C\sigma_{Mz}$	Sh
21	1.054	0.141	-0.013	0.432	-0.012	0.045	-
3	1.049	0.140	-0.093	0.907	0.002	0.084	-
7	1.118	0.157	0.106	0.799	0.009	0.082	-
13	1.054	0.096	-0.013	0.533	-0.004	0.052	-
6	1.090	0.169	-0.013	1.138	-0.013	0.090	0.100
5	1.102	0.171	-0.043	1.122	0.008	0.095	0.099
18	0.998	0.041	0.023	0.553	-0.006	0.042	0.095
9	1.045	0.082	-0.033	0.541	-0.003	0.050	0.129
15	1.084	0.103	0.148	0.425	0.006	0.044	0.173
10	1.072	0.108	0.023	0.403	-0.005	0.045	0.173
Yu&Kareem (2006, 2011) [4]	1.176	~0.1	~0.05	~1	-	-	-
Schewe (2006, 2009) [5]	1.029	-	0.0	~0.4	-	-	0.111

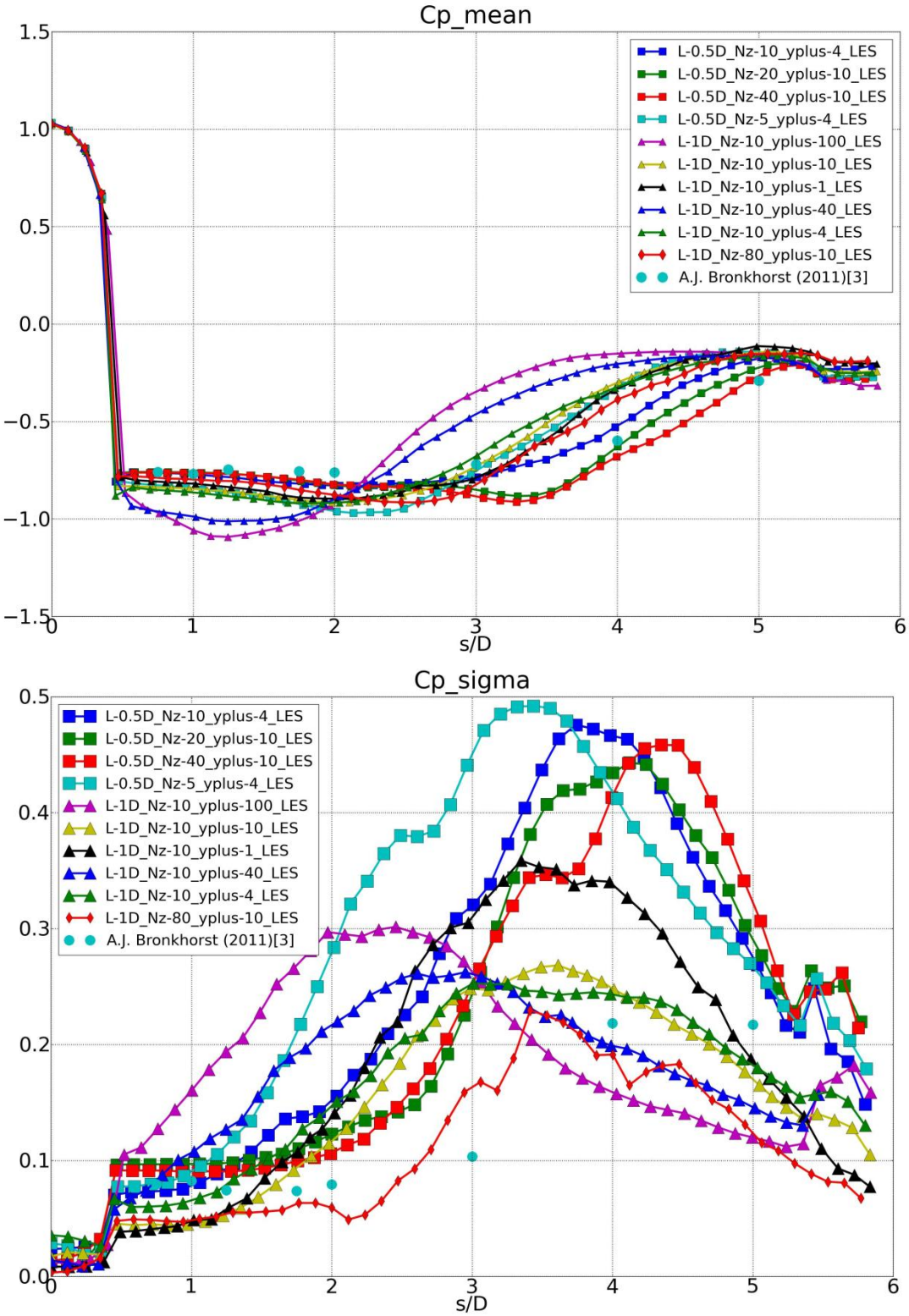

Figure 2: LES simulations. Mean ,C_p, (top) and standard-deviation, $C_{\sigma p}$, (bottom) values distribution of pressure coefficients. In legend from the top to the bottom: Case 3, Case 5, Case 6, Case 7, Case 10, Case 9, Case 21, Case 15, Case 13, Case 18, Experiment [3]

5.2 DES simulations

The obtained results of DES simulations are presented in Table 3 and Figures 3.

The investigations showed that big values of y+ (more than 40) lead to underestimation of maximum values of $C_{\sigma p}$ due to poor mesh resolution in LES region. Too small values of y+ (less than 30) lead to overestimation of maximum values of $C_{\sigma p}$. Irregularity of cell shape (ratio_zx≥58, ratio_zy≥58) and incorrect wall function operation probably impact on the $C_{\sigma p}$ distribution.

The size of domain in the transverse direction (Z) does not influence significantly on the results. L=1D is optimal in terms of computational cost and reliability of results.

The main aerodynamic integral parameters (Table 3) seem not to be sensitive to grid resolution and are similar to the other studies [4, 5].

Table 3: Mean (C_D, C_L), standard-deviation ($C\sigma_D$, $C\sigma_L$) and Strouhal number (Sh) values of drag and lift coefficients for several DES simulations

Case Number	C_D	$C\sigma_D$	C_L	$C\sigma_L$	C_{Mz}	$C\sigma_{Mz}$	Sh
2	1.011	0.176	0.149	0.979	-0.014	0.109	0.100
12	1.142	0.060	0.077	1.091	0.006	0.083	0.122
8	1.134	0.048	0.033	1.049	0.006	0.079	0.122
11	1.106	0.027	0.057	0.927	0.007	0.069	0.122
1	1.250	0.221	-	1.505	0.184	0.116	0.133
4	1.027	0.252	0.189	1.568	0.029	0.119	0.097
14	1.078	0.021	-0.005	0.778	0.001	0.057	0.123
17	1.009	0.162	-0.229	1.170	-0.005	0.098	0.121
19	1.083	0.020	-0.009	0.781	0.001	0.058	0.123
20	1.084	0.017	-0.006	0.782	0.002	0.058	0.124
16	1.069	0.022	-0.002	0.748	0.002	0.055	0.124
Yu&Kareem (2006, 2011) [4]	1.176	~0.1	~0.05	~1	-	-	-
Schewe (2006, 2009) [5]	1.029	-	0.0	~0.4	-	-	0.111

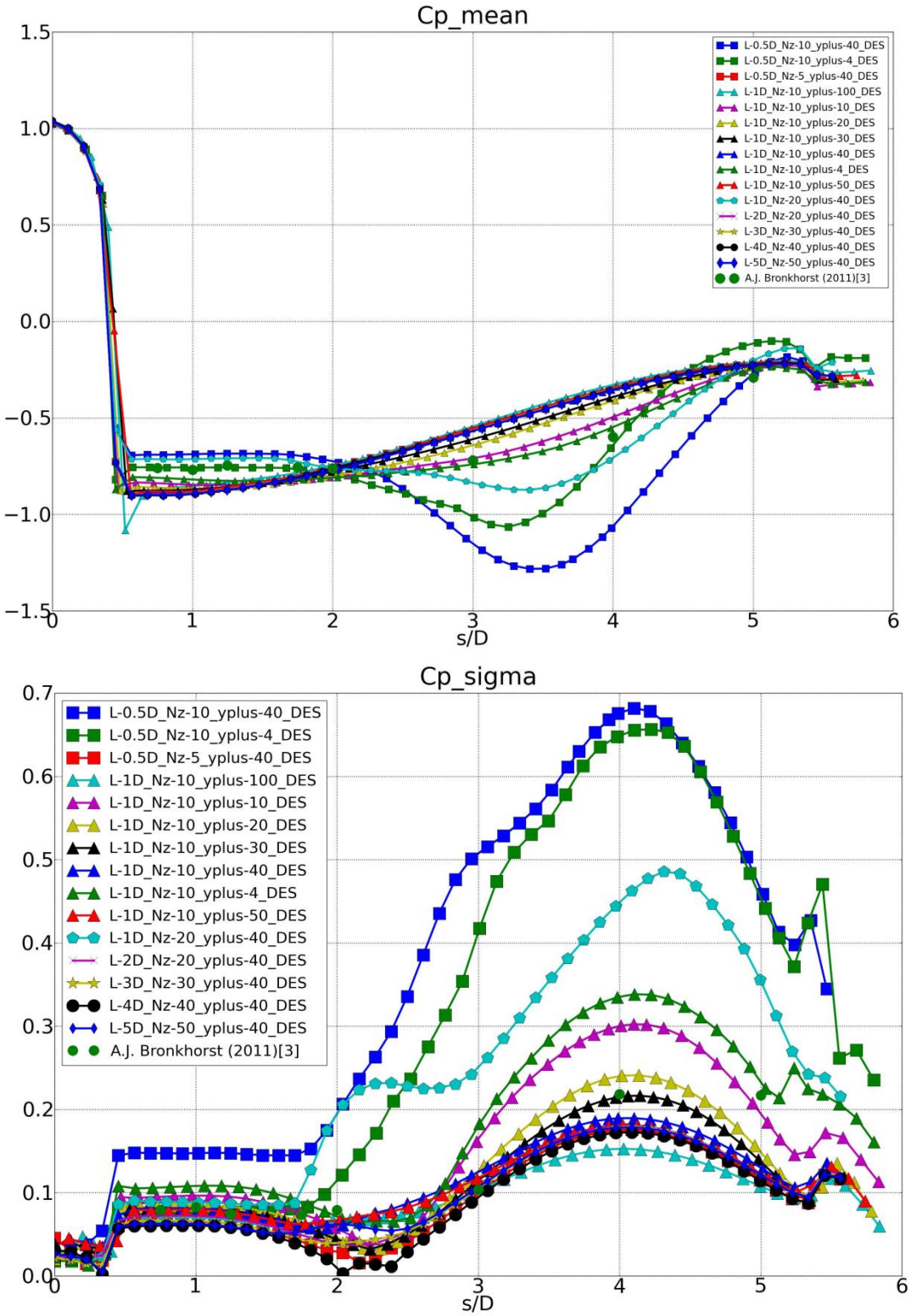

Figure 3: DES simulations. Mean ,C_p, (top) and standard-deviation, $C_{\sigma p}$, (bottom) values distribution of pressure coefficients. In legend from the top to the bottom: Case 4, Case 2, Case 22, Case 23, Case 8, Case 11, Case 24, Case 14,Case 12, Case 1, Case 17, Case 25, Case 26, Case 19, Case 20, Experiment [3]

5.3 Results closest to experiment

The most accurate simulation cases was chosen for LES and DES turbulence models. Appropriate mesh parameters was found out (Case 14 for DES, Case 18 for LES – see Table 1). The results for these cases are presented below (Table 4, Figure 4).

Table 4: Mean (C_D, C_L), standard-deviation ($C\sigma_D$, $C\sigma_L$) and Strouhal number (Sh) values of drag and lift coefficients

Case Number	C_D	$C\sigma_D$	C_L	$C\sigma_L$	C_{Mz}	$C\sigma_{Mz}$	Sh
14 (DES)	1.078	0.021	-0.005	0.778	0.001	0.057	0.123
18 (LES)	0.998	0.041	0.023	0.553	-0.006	0.042	0.095
Yu&Kareem (2006, 2011) [4]	1.176	~0.1	~0.05	~1	-	-	-
Schewe (2006, 2009) [5]	1.029	-	0.0	~0.4	-	-	0.111

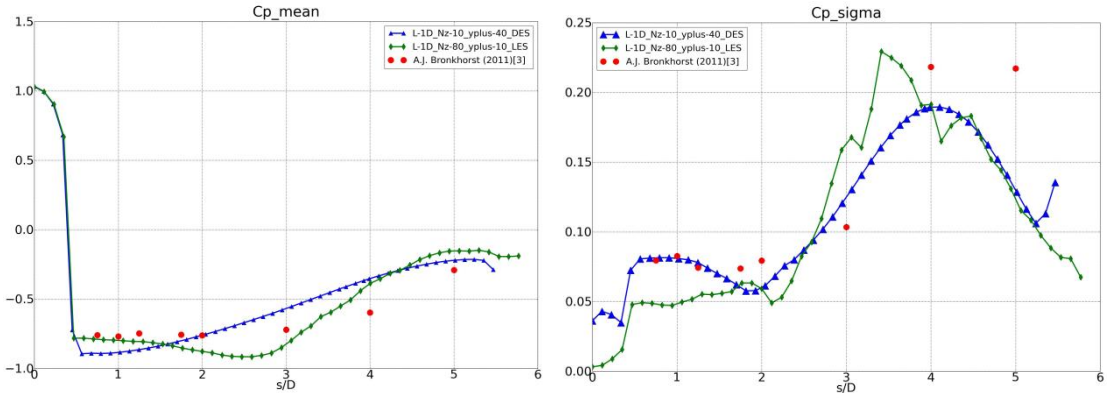

Figure 4: Mean ,C_p, (right) and standard-deviation, $C_{\sigma p}$, (left) values distribution of pressure coefficients. In legend from the top to the bottom: Case 14 (DES), Case 18 (LES), Experiment [3]

The obtained results showed that LES turbulence model is fairly heavy for application – the mesh must be very fine (Number of cells = 8e+006 for Case 18) to obtain consistent results while the DES model requirement is 10 times less than LES model (Number of cells = 6e+005 for Case 14). This kind of research gave understanding of "the cost" of the obtaining authentic results using LES approach, the limit of the mesh simplification near and around the body for DES approach.

6 CONCLUSIONS

- The multivariate verification investigations of the influence of the grid resolution in the boundary layer (near the walls of the rectangular), in the transverse direction (Z) to the cross section and the influence of the domain size in the transverse direction (Z) on the results were carried out at the world-known benchmark BARC [2], that is devoted to 1:5 prism aerodynamics research.
- The assess of the applicability of LES (Large Eddy Simulation) and DES (Detached

Eddy Simulation) turbulence models for solving the concerned class of problems was performed.

- The significant dependence numerical results on grid resolution in the boundary layer (especially for LES), on the aspect ratio of the elements edges (in three directions), on the size of domain in the transverse direction to the cross section of structure and on the domain size in the transverse direction (Z) was obtained.
- The most appropriate mesh parameters was found out.
- The obtained results showed that LES turbulence model is fairly heavy for application at real buildings and structures – the mesh must be very fine to obtain consistent results while the DES model requirement is 10 times less than LES model. Therefore DES model is far more suitable for the application to the civil problems – including the bridge and high-rise buildings aerodynamics investigation.
- This technique is supposed to be applied to the simplified bridge model (a rectangular with aspect ratio 1:10 in bridge true scale and with imposed appropriate boundary conditions) and to the real complex bridge model. The numerical results will be compared with experimental data from the wind tunnel. The purpose of this research is to estimate practicability of the two-dimensional/quasi-two-dimensional simulation versus to the three-dimensional simulation of the bridge deck aerodynamics and to clarify the developed recommendations for more complex structures than a rectangular cylinder.
- The considered problems is to be solved using Fluid Structure Interface (FSI) methods.

REFERENCES

[1] ANSYS, Inc. (2013), "ANSYS 14.5 Help".

[2] L. Bruno, D. Fransos, N. Coste, and A. Bosco, 3D flow around a rectangular cylinder: a computational study, *BBAA* VI *Colloquium on: Bluff Bodies Aerodynamics & Applications*, Proceedings, Milano, Italy, July, 20-24 2008.

[3] A.J. Bronkhorst, C.P. Geurts, C.A. van Bentum, Unsteady pressure measurements on a 5:1 rectangular cylinder. *13th International Conference on Wind Engineering*, Proceedings, July 10-15, 2011.

[4] Z. Wei, A. Kareem, A benchmark study of flow around a rectangular cylinder with aspect ratio 1:5 at Reynolds number 1.E5. *13th International Conference on Wind Engineering*, Proceedings, July 10-15, 2011.

[5] C. Mannini, G. Schewe, Numerical study on the three-dimensional unsteady flow past a 5:1 rectangular cylinder using the DES approach. *13th International Conference on Wind Engineering*, Proceedings, July 10-15, 2011.

[6] L. Bruno, D. Fransos, N. Coste, A. Bosco, 3D Flow around a rectangular cylinder: a computational study. *13th International Conference on Wind Engineering*, Proceedings, July 10-15, 2011.